Cleavage of an Amide Bond by a Ribozyme

Xiaochang Dai, Alain De Mesmaeker, Gerald F. Joyce*

A variant form of a group I ribozyme, optimized by in vitro evolution for its ability to catalyze magnesium-dependent phosphoester transfer reactions involving DNA substrates, also catalyzes the cleavage of an unactivated alkyl amide when that linkage is presented in the context of an oligodeoxynucleotide analog. Substrates containing an amide bond that joins either two DNA oligos, or a DNA oligo and a short peptide, are cleaved in a magnesium-dependent fashion to generate the expected products. The first-order rate constant, k_{cat}, is 0.1×10^{-5} min^{-1} to 1×10^{-5} min^{-1} for the DNA-flanked substrates, which corresponds to a rate acceleration of more than 10^3 as compared with the uncatalyzed reaction.

All of the RNA enzymes (ribozymes) that are known to exist in nature carry out phosphoester cleavage or phosphoester transfer reactions involving RNA substrates. A notable exception may prove to be 23S ribosomal RNA from *Thermus aquaticus*, which likely catalyzes the formation of an amide bond between an aminoacyl oligonucleotide and the aminoacyl nucleoside analog puromycin (*1*). It has not been possible, however, to carry out this reaction in the complete absence of protein.

Since the discovery of ribozymes in nature (*2*), there has been considerable interest in exploring the catalytic potential of RNA in the laboratory. A broad functional capacity seems plausible not only on chemical grounds but also in light of the presumed role of RNA during the early history of life on Earth (*3*, *4*). Cech and co-workers have shown that the *Tetrahymena* group I ribozyme, which normally catalyzes phosphoester transfer reactions involving RNA substrates, can be made to accelerate the hydrolysis of a carboxyester 5- to 15-fold when that linkage is presented in the context of an aminoacyl oligonucleotide (*5*). The development of in vitro selection and in vitro evolution methodology promises to further expand the known repertoire of RNA enzymes (*6*). Recently, for example, Schultz and co-workers generated an RNA enzyme that catalyzes the interconversion of two rotational isomers of a hindered biphenyl compound, accelerating this process about 100-fold (*7*).

The *Tetrahymena* group I ribozyme catalyzes the sequence-specific cleavage of RNA substrates by a Mg^{2+}-dependent phosphoester transfer mechanism (*8*). The reaction involves nucleophilic attack by guanosine 3′-hydroxyl at a specific phosphodiester linkage within the ribozyme-bound substrate. Binding specificity derives from Watson-Crick base pairing between a template domain that lies near the 5′ end of

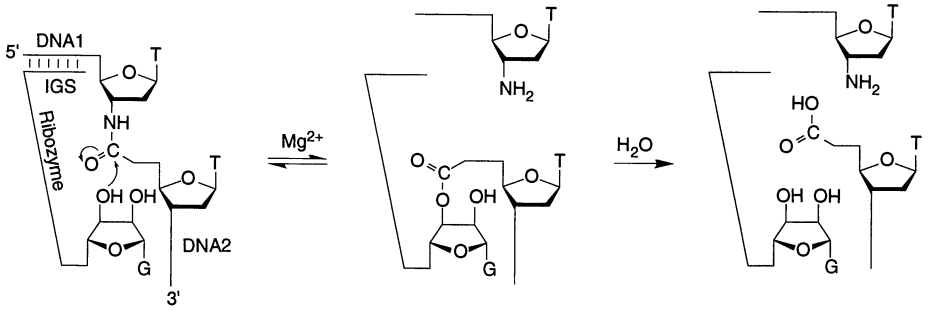

Fig. 1. Proposed scheme for RNA-catalyzed amide cleavage. Hybridization of the ribozyme's IGS (3′-GGGAGG-5′) to DNA1 (5′-CCCTCT-3′) positions the amide in close proximity to the ribozyme's 3′-terminal guanosine. Nucleophilic attack by G_{OH} on the carbonyl carbon of the substrate, in the presence of Mg^{2+}, results in release of DNA1 (terminated by a 3′ amine) and esterification of the ribozyme to DNA2. The carboxyester intermediate is expected to undergo spontaneous hydrolysis, releasing DNA2 (terminated by a 5′ carboxyl) and allowing turnover of the ribozyme. Substrates were prepared by solid-phase synthesis, with the use of standard phosphoramidite chemistry (*26*); the amide linkage was provided in the context of a thymidine dimer (*17*). 5′-Dimethoxytrityl substrates were purified by reversed-phase high-pressure liquid chromatography, deprotected, then further purified by denaturing PAGE and reversed-phase chromatography (DuPont NENsorb). Ribozymes were prepared by in vitro transcription (*12*). The evolved ribozyme in this study (generation 27, clone 48) (*12*) contained 17 mutations relative to the wild-type *Tetrahymena* ribozyme: 44: G → A; 51/52: insert AGAA; 87: A → delete; 94: A → U; 115: A → U; 116: G → A; 166: C → A; 170: C → U; 188: G → A; 190: U → A; 191: G → U; 205: U → C; 215: G → A; 239: U → A; 312: G → A; 350: C → U; and 364: C → U.

4. Biotin was attached to the 3′ end of tRNA by means of a hydrazide linkage. The *E. coli* $tRNA^{Phe}$ (3 nmol) was reacted with 40 mM KIO_4 for 1 hour in the dark at room temperature in a volume of 100 μl. After the reaction was stopped by addition of 100 μl of 50% ethylene glycol, the oxidized tRNA was precipitated with ethanol, redissolved in 100 μl of 10 mM biotin-amidocaproyl hydrazide (Sigma), and incubated for 2 hours at 37°C. The resulting hydrazone was reduced to the hydrazide by addition of 100 μl of 0.2 M $NaBH_4$ and 200 μl of 1 M tris-HCl (pH 8.2), followed by incubation for 30 min in the dark on ice. Biotin-derivatized tRNA was purified from reactants with a 1-ml Sephadex G-50 spin column. The *E. coli* 30S ribosomal subunits (90 pmol), prepared as described (*2*), were incubated with 20 μg of poly(U) at 37°C for 5 min (where indicated), followed by incubation with 70 pmol of biotinylated $tRNA^{Phe}$ for 20 min at 37°C and then for 20 min on ice, in a buffer containing 50 mM tris-HCl (pH 7.5), 150 mM NH_4Cl, 1 mM dithiothreitol, and 6 to 25 mM $MgCl_2$, according to the experiment, in a total volume of 300 μl. We captured active 30S subunits by incubating them for 10 min at room temperature with 100 μl of a suspension of magnetic streptavidin beads (10 mg/ml; streptavidin-M280; Dynal) prewashed with buffer containing 0.3% bovine serum albumin, and the unbound subunits were removed by washing three times with buffer after the beads were trapped with a magnet. Bound subunits were released by addition of 200 μl of 5 mM EDTA, 0.5% SDS, 300 mM sodium acetate (pH 6.0), and the RNA extracted as described (*8*). Chemical modification with kethoxal, dimethylsulfide (DMS), or 1-cyclohexyl-3-(2-morpholinoethyl)carbodiimide metho-*p*-toluenesulfonate (CMCT) was carried out for 10 min at 37°C and assayed by primer extension as described (8). Levels of modification were quantified with a PhosphorImager (Molecular Dynamics). After normalization to account for differences in lane loadings, background levels estimated from unmodified sample lanes were subtracted, and the resulting value for a given base position was calculated as a fraction of the modification level measured for that base in the total modified subunit pool.
5. S. Rose III, P. Lowary, O. Uhlenbeck, *J. Mol. Biol.* **167**, 103 (1983).
6. A. Hüttenhofer and H. Noller, *Proc. Natl. Acad. Sci. U.S.A.* **89**, 7851 (1992).
7. S. Kirrilov, V. Makhno, Y. Semenkov, *Nucleic Acids Res.* **8**, 183 (1980).
8. S. Stern, D. Moazed, H. Noller, *Methods Enzymol.* **164**, 481 (1988).
9. We also observed strong interference by kethoxal modification of position G1338 in mRNA-independent tRNA binding (Fig. 2). However, this interference effect was not observed with all ribosome preparations. Previously, G1338 was found to be protected from kethoxal modification by P site tRNA (*2*), and similarly, some unexplained variability in protection was seen at this position among different ribosome preparations.
10. S. Stern, B. Weiser, H. Noller, *J. Mol. Biol.* **204**, 447 (1988).
11. P. Gornicki, K. Nurse, W. Hellmann, M. Boublik, J. Ofengand, *J. Biol. Chem.* **259**, 10493 (1984); T. Wagenknecht, J. Frank, M. Boublik, K. Nurse, J. Ofengand, *J. Mol. Biol.* **203**, 753 (1988).
12. U. von Ahsen and H. F. Noller, unpublished results.
13. N. Larsen *et al.*, *Nucleic Acids Res.* **21** (suppl.), 3021 (1993).
14. J. Prince, B. Taylor, D. Thurlow, J. Ofengand, R. Zimmerman, *Proc. Natl. Acad. Sci. U.S.A.* **79**, 5450 (1982); R. Denman, J. Colgan, K. Nurse, J. Ofengand, *Nucleic Acids Res.* **16**, 165 (1988).
15. P. Cunningham, K. Nurse, C. Weitzmann, D. Negre, J. Ofengand, *Biochemistry* **31**, 7629 (1992).
16. W. Herr, N. Chapman, H. Noller, *J. Mol. Biol.* **130**, 433 (1979).
17. This work was supported by NIH grant #GM17129 (to H.F.N.), a long-term fellowship to U.v.A. from the European Molecular Biology Organization, and a grant to the Center for Molecular Biology of RNA from the Lucille P. Markey Charitable Trust. We thank B. Singaram, R. Green, I. Lee, and C. Merryman for helpful discussions.

27 July 1994; accepted 28 October 1994

the ribozyme (the internal guide sequence or IGS) and substrate nucleotides located on the 5′ side of the cleavage site. In addition, the ribozyme forms tertiary contacts with the IGS-substrate duplex, adding 4 kcal mol^{-1} of binding energy and positioning the substrate in close proximity to the guanosine nucleophile (9). When provided with a DNA rather than RNA substrate, the ribozyme cannot form these tertiary contacts and its catalytic efficiency (k_{cat}/K_m) is reduced from 1×10^7 M^{-1} min^{-1} for RNA to 40 M^{-1} min^{-1} for DNA (*10*, *11*).

In previous work, we applied an in vitro evolution procedure to a large population of *Tetrahymena* ribozyme variants to obtain molecules that catalyzed sequence-specific DNA cleavage with 10^5-fold improved efficiency as compared with that of the wild-type ribozyme (*11*, *12*). The evolved ribozymes had developed novel tertiary contacts that provided 5 kcal mol^{-1} of binding energy beyond what could be attributed to IGS-substrate base-pairing interactions. They retained the ability to cleave RNA with high efficiency ($k_{cat}/K_m = 3 \times 10^7$ M^{-1} min^{-1}). When provided with a DNA substrate that contained a single arabinonucleoside at the cleavage site, the evolved, but not the wild-type, ribozymes catalyzed efficient substrate cleavage ($k_{cat}/K_m = 3 \times 10^7$ M^{-1} min^{-1}) (*13*). The DNA-cleavage reaction required that the sequence 5′ of the cleavage site be complementary to the IGS but was not constrained by the sequence 3′ of the cleavage site (*14*). Thus, the evolved ribozymes were able to react with a variety of substrates, so long as they contained a target pentose-phosphate located immediately downstream from a region that could form stable Watson-Crick pairs with the IGS.

Because the phosphate ground state and the transition state for amide hydrolysis have a similar tetrahedral geometry, we reasoned that the ability of the evolved ribozymes to target phosphate esters in the context of a nucleic acid substrate might facilitate cleavage of carboxamides in the same context. The catalytic Mg^{2+}, which has a demonstrated role in stabilizing the 3′-alkoxy leaving group during phosphoester cleavage (*15*) and a likely role in coordinating to a nonbridging phosphate oxygen (*16*), might play analogous roles in stabilizing the 3′-NH_2 leaving group and coordinating to the carbonyl oxygen during amide cleavage. To test this hypothesis, we prepared an oligodeoxynucleotide analog substrate containing a 3′-NH-CO-CH_2-5′ linkage (*17*) at the desired cleavage site, located between an upstream sequence [5′-GGCCCTCT-3′ (DNA1)] that can form base pairs with the ribozyme IGS and a downstream sequence [5′-TAA$(TAAA)_3$-3′ (DNA2)] that will be transferred to the nucleophilic guanosine 3′-hydroxyl as a consequence of amide cleavage (Fig. 1).

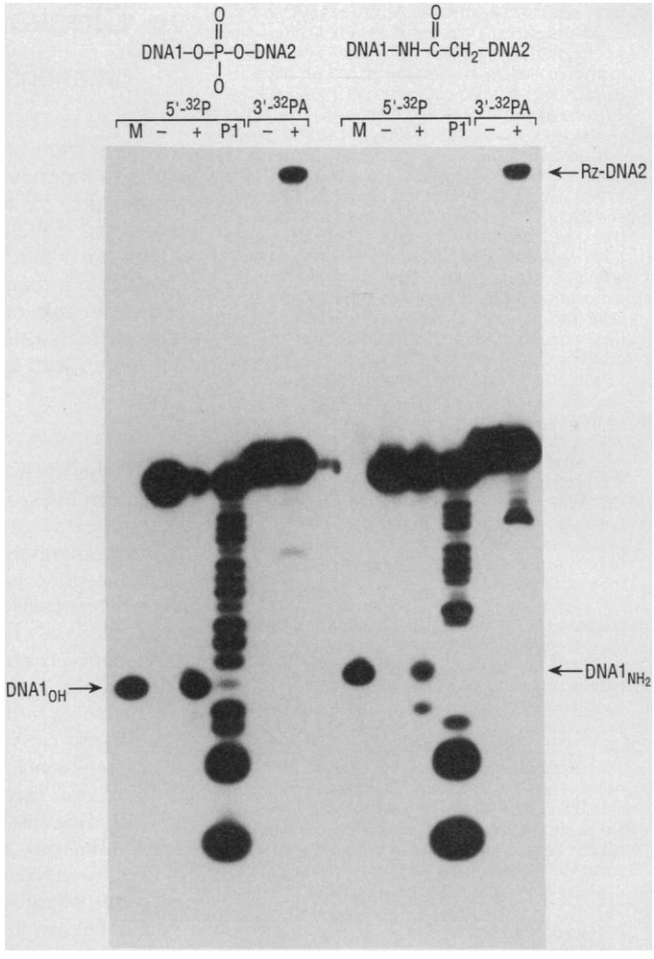

Fig. 2. RNA-catalyzed cleavage of phosphodiester- and amide-linked substrates. Substrates were 5′ labeled with the use of T4 polynucleotide kinase and [γ-^{32}P]ATP or 3′ labeled with the use of terminal deoxynucleotidyl transferase and [α-^{32}P]ddATP (indicated by ^{32}PA) (*11*). Authentic $DNA1_{OH}$ and $DNA1_{NH_2}$ were similarly 5′ labeled and served as markers (lane M) for the expected 5′-cleavage products. $DNA1_{NH_2}$ was prepared from d(GGCCCTC) by enzymatic addition of T_{NH_2} [reaction conditions: 175 μM synthetic DNA oligo, 1 mM 3′-amino-3′-deoxythymidine-5′-triphosphate, terminal transferase (3.4 U μl^{-1}), 100 mM sodium cacodylate (pH 7.2), 2 mM $CoCl_2$, and 2 mM 2-mercaptoethanol, incubated at 37°C for 1 hour]. Labeled substrates and markers were purified by denaturing PAGE and reversed-phase chromatography. Minus signs, unincubated; plus signs, incubated in the presence of ribozyme. $DNA1_{NH_2}$ migrates slightly more slowly than does $DNA1_{OH}$ because the terminal amine ($pk_a \approx 8.1$, determined for 3′-amino-2′,3′-dideoxythymidine by ^{13}C-NMR spectroscopy) is partially protonated under the gel electrophoresis conditions (pH 8.3). Reaction conditions: 1.0 μM ribozyme, 1.0 μM substrate, 10 mM $MgCl_2$, and 30 mM EPPS (pH 7.5) at 37°C, incubated for 20 min for phosphodiester substrate or 18 hours for amide substrate. P1 nuclease ladders (lane P1) were obtained by partial digestion of 5′-labeled substrate [reaction conditions: 0.3 μM substrate, P1 nuclease (2×10^{-4} U μl^{-1}), 0.1 mM $ZnCl_2$, and 10 mM sodium acetate (pH 5.2), incubated at 50°C for 10 min]. P1 nuclease does not cleave the amide bond or the phosphodiester linkages that lie one nucleotide upstream or downstream from the amide. Reaction products were separated by electrophoresis in a 20% polyacrylamide–8 M urea gel, an autoradiogram of which is shown. Rz-DNA2 denotes the expected position of ribozyme that is covalently linked to DNA2.

Incubation of [5′-^{32}P]-labeled amide-containing substrate with the evolved ribozyme and $MgCl_2$ generated two labeled products that co-migrated with authentic [5′-^{32}P]G-GCCCTCT$_{NH_2}$ and [5′-^{32}P]GGCCCTC$_{OH}$ (Fig. 2). Incubation of [3′-^{32}P-A]-labeled amide-containing substrate under the same conditions generated two labeled products: one that migrated slightly more slowly than the ribozyme and the other of the expected length for $_{HOOC}$TAA$(TA_3)_3$[3′-^{32}P-A] (Fig. 2). No 5′ or 3′ cleavage products were detected when the amide-containing substrate was incubated without ribozyme or with the wild-type *Tetrahymena* ribozyme. Precautions were taken to ensure that the observed activity was not due to a contaminating protease or amidase protein (*18*).

The purified 5′ cleavage product and authentic $DNA1_{NH_2}$ were equally reactive with ninhydrin, which is consistent with the presence of a primary amine; whereas intact amide-containing substrate and $DNA1_{OH}$ were nonreactive. We used sulfosuccinimidyl-6-(biotinamido) hexanoate, which forms a stable covalent adduct with primary amines, to modify the 5′ cleavage product and authentic $DNA1_{NH_2}$ in a side-by-side manner (Fig. 3). For both compounds, the apparent rate constant k_{obs} for the deriva-

X. Dai and G. F. Joyce, Departments of Chemistry and Molecular Biology, The Scripps Research Institute, 10666 North Torrey Pines Road, La Jolla, CA 92037, USA.
A. De Mesmaeker, Central Research Laboratories, Ciba-Geigy Limited, Basel, Switzerland.
*To whom correspondence should be addressed.

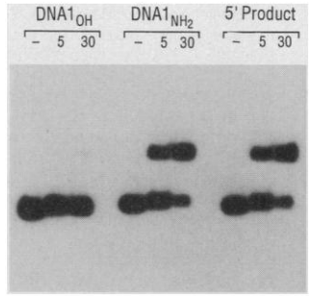

Fig. 3. Characterization of the products of RNA-catalyzed amide cleavage. Authentic [5′-^{32}P]DNA1$_{NH_2}$ and [5′-^{32}P]DNA1$_{OH}$ as well as the slower-migrating 5′ product obtained by RNA-catalyzed cleavage of [5′-^{32}P]DNA1$_{NHCOCH_2}$DNA2 were covalently modified and subjected to gel-shift analysis. Labeled compounds were purified by denaturing PAGE and reversed-phase chromatography before derivatization. Reaction conditions: 1 nM DNA oligo, 30 mM sulfosuccinimidyl-6-(biotinamido) hexanoate (Pierce Chemical), and 100 mM $NaHCO_3$ (pH 8.5), incubated at 25°C for 5 or 30 min. Reaction products were separated by electrophoresis in a 20% polyacrylamide–8 M urea gel, an autoradiogram of which is shown. The slower-migrating species corresponds to covalent addition of 6-biotinamido hexanoate to the primary amine of DNA1$_{NH_2}$. Values for k_{obs} were obtained by replicate time-course experiments under these reaction conditions; reactions were followed for more than three half-lives.

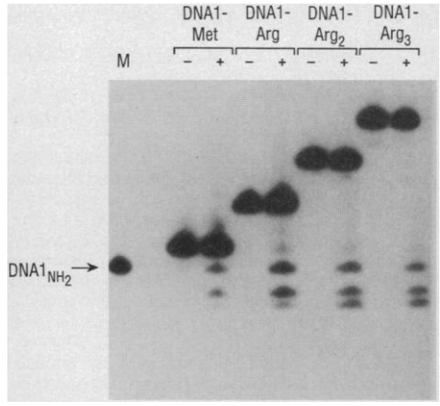

Fig. 4. RNA-catalyzed cleavage of DNA1-Met or DNA1-Arg$_n$ (n = 1, 2, or 3). Reaction conditions: 0.5 nM [5′-^{32}P]-labeled substrate, 10 mM $MgCl_2$, and 30 mM EPPS (pH 7.5), incubated at 37°C for 18 hours in the absence (minus sign) or presence (plus sign) of 0.5 μM ribozyme. Reaction products were separated by electrophoresis in a 20% polyacrylamide–8 M urea gel, an autoradiogram of which is shown. Lane M, authentic [5′-^{32}P]-DNA1$_{NH_2}$.

tization reaction at pH 8.5 was 0.033 ± 0.005 min^{-1}. On this basis, we concluded that the slower-migrating 5′ cleavage product was indeed GGCCCTCT$_{NH_2}$.

The rate of RNA-catalyzed amide cleavage was slow, only 1×10^{-6} min^{-1} at pH 7.5 and 37°C (*19*). Nonetheless, this is about 10^3 times faster than that of the uncatalyzed reaction, which is undetectable in our system ($k_{uncat} < 6 \times 10^{-9}$ min^{-1}) but is expected to be less than 10^{-9} min^{-1} on the basis of the rate of hydrolysis of *N*-methylacetamide at pH 7.5 and 25°C (*20*). A slightly different amide-containing substrate, in which the downstream sequence was changed from 5′-TAA(TAAA)$_3$-3′ to 5′-TAG(TAAA)$_3$-3′, was cleaved somewhat faster ($k_{cat} = 1 \times 10^{-5}$ min^{-1}).

The RNA-catalyzed amide cleavage reaction was absolutely dependent on Mg^{2+}. A trace amount of cleavage was observed in the presence of 10 mM $MnCl_2$, in contrast to the RNA and DNA cleavage reactions, which proceed readily in $MnCl_2$. No amide cleavage was detected in the presence of Zn^{2+}, Ca^{2+}, or Sr^{2+}. The Mg^{2+}-dependent reaction was optimal in the presence of 20 mM $MgCl_2$ and was not accelerated by the addition of 0.1 to 1 mM $ZnCl_2$.

We were unable to isolate the putative acyl intermediate in the amide cleavage reaction, because its electrophoretic mobility was nearly identical to that of the phosphoester transfer product resulting from miscleavage one nucleotide upstream of the amide. When we used a truncated form of the ribozyme lacking the 3′-terminal guanosine and supplied the nucleophile in the form of free guanosine, there was no detectable substrate cleavage. However, three indirect pieces of evidence point to the existence of the acyl intermediate. First, RNA-catalyzed cleavage of the 3′-labeled amide-containing substrate produced a slowly migrating species corresponding in length to the ribozyme-DNA2 adduct (Fig. 2). Second, the 5′ products resulting from cleavage of the amide-containing and all-DNA substrates were present in nearly equal amounts, whereas the free 3′ cleavage products, presumably $_{HOOC}$TAA(TAAA)$_3$[3′-^{32}P-A] and pTAA(TAAA)$_3$[3′-^{32}P-A], were present in unequal amounts; the larger amount of the former likely reflects the more facile hydrolysis of the acyl intermediate as compared with the phosphoester intermediate. Third, incubation of unlabeled amide-containing substrate with the evolved ribozyme and authentic [5′-^{32}P]DNA1$_{NH_2}$ generated full-length 5′-labeled substrate, which is indicative of amide bond formation. This reaction, which did not occur with the mismatched substrate [5′-^{32}P]AGCGGTT$_{NH_2}$, likely involves attack of [5′-^{32}P]DNA1$_{NH_2}$ on the unlabeled acyl intermediate.

To explore the generality of the RNA-catalyzed amide cleavage reaction, we prepared a series of substrates in which an amino acid or short peptide was appended to DNA1 by an amide linkage (*21*). Of four substrates tested, DNA1-Met and DNA1-(Arg)$_n$ (n = 1, 2, or 3) all were cleaved by the ribozyme at the amide linkage immediately after DNA1 as well as at the phosphodiester linkage one nucleotide upstream from the amide (Fig. 4). No cleavage was observed at the peptide linkages within the (Arg)$_2$- and (Arg)$_3$-containing substrates.

Amide-cleavage reactions have been carried out with other synthetic macromolecular catalysts, including catalytic antibodies that hydrolyze an activated amide (*22*) or a peptide bond in the presence of a reactive Zn(II) complex (*23*). Most recently, a catalytic antibody against a dialkylphosphinate transition-state analog was found to cleave an unsubstituted amide, in the absence of a cofactor, with $k_{cat} \approx 10^{-5}$ min^{-1} at pH 9.0 and 37°C (*24*).

The amide-cleaving ribozymes used in this study were the product of in vitro evolution for phosphoester transferase activity. We hypothesize that their ability to cleave amides is related to the similar structural and electronic features of the ground-state phosphate and the transition state for amide hydrolysis. Alternatively, one could view this as an example of crossover catalysis on the basis of the similar mechanistic features of the two reactions. It has been suggested that an ancestral ribozyme, perhaps akin to a group I intron, catalyzed both RNA polymerization and peptide bond formation (*4*, *25*). We are hesitant to ascribe primordial character to the amide-cleaving ribozymes—they are the contemporary products of biological evolution, enhanced by evolution in the laboratory. Nonetheless, it is striking that a single ribozyme is able to cleave RNA and DNA phosphodiesters as well as amide bonds.

REFERENCES AND NOTES

1. H. F. Noller, V. Hoffarth, L. Zimniak, *Science* **256**, 1416 (1992).
2. K. Kruger *et al.*, *Cell* **31**, 147 (1982); C. Guerrier-Takada, K. Gardiner, T. Marsh, N. Pace, S. Altman, *ibid.* **35**, 849 (1983).
3. W. Gilbert, *Nature* **319**, 618 (1986); G. F. Joyce, *ibid.* **338**, 217 (1989); S. A. Benner, A. D. Ellington, A. Tauer, *Proc. Natl. Acad. Sci. U.S.A.* **86**, 7054 (1989).
4. A. M. Weiner and N. Maizels, *Proc. Natl. Acad. Sci. U.S.A.* **84**, 7383 (1987).
5. J. A. Piccirilli, T. S. McConnell, A. J. Zaug, H. F. Noller, T. R. Cech, *Science* **256**, 1420 (1992).
6. For recent reviews, see G. F. Joyce, *Curr. Opin. Struct. Biol.* **4**, 331 (1994); R. R. Breaker and G. F. Joyce, *Trends Biotechnol.* **12**, 268 (1994); and K. B. Chapman and J. W. Szostak, *Curr. Opin. Struct. Biol.* **4**, 618 (1994).
7. J. R. Prudent, T. Uno, P. G. Schultz, *Science* **264**, 1924 (1994).
8. A. J. Zaug, M. D. Been, T. R. Cech, *Nature* **324**, 429 (1986).
9. A. M. Pyle and T. R. Cech, *ibid.* **350**, 628 (1991); P. C. Bevilacqua and D. H. Turner, *Biochemistry* **30**, 10632 (1991); A. M. Pyle, F. L. Murphy, T. R. Cech, *Nature* **358**, 123 (1992); D. Herschlag, F. Eckstein, T. R. Cech, *Biochemistry* **32**, 8299 (1993).
10. D. Herschlag and T. R. Cech, *Nature* **344**, 405 (1990).
11. A. A. Beaudry and G. F. Joyce, *Science* **257**, 635 (1992).
12. J. Tsang and G. F. Joyce, *Biochemistry* **33**, 5966 (1994).
13. ———, unpublished results.

14. S.-A. Raillard, A. Banerji, G. F. Joyce, unpublished results.
15. J. A. Piccirilli, J. S. Vyle, M. H. Caruthers, T. R. Cech, *Nature* **361**, 85 (1993).
16. T. R. Cech, *J. Biol. Chem.* **267**, 17479 (1992); T. A. Steitz and J. A. Steitz, *Proc. Natl. Acad. Sci. U.S.A.* **90**, 6498 (1993).
17. J. Lebreton *et al.*, *Tetrahedron Lett.* **34**, 6383 (1993).
18. Four different preparations of the evolved ribozyme, purified by two phenol extractions, chloroform-isoamyl alcohol extraction, high-resolution denaturing polyacrylamide gel electrophoresis (PAGE), and reversed-phase chromatography (DuPont NENsorb), all exhibited comparable amounts of activity. This activity was lost after incubation with ribonuclease A but was retained after phenol extraction or incubation with proteinase K.
19. The k_{cat} was obtained at a saturating concentration of ribozyme with ribozyme in excess over substrate. Reaction conditions were either 50 nM substrate and 0.5, 1.0, or 2.0 μM ribozyme, or 60 nM substrate and 0.3 or 0.6 μM ribozyme, incubated in the presence of 10 mM $MgCl_2$ and 30 mM *N*-[2-hydroxymethyl]-piperazine-*N*′-[3-propanesulfonic acid] (pH 7.5) at 37°C for 2, 6, or 18 hours. The rate of product formation was linear over the reaction ($r > 0.99$). Product accounted for less than 10% of the starting material, even at the highest ribozyme concentration and latest time point, which allowed us to neglect loss of starting material due to cleavage at the phosphodiester linkage following GGCCCTC. A plot of reaction velocity versus ribozyme concentration was linear ($r = 0.999$), the slope providing an estimate for k_{cat} of $1 \pm 0.3 \times 10^{-6}$ min^{-1}.
20. The uncatalyzed reaction was evaluated by incubation of 50 nM (7.7×10^5 cpm) [5′-^{32}P]-labeled substrate under the standard reaction conditions for 86 hours and analysis of the products with a PhosphorImager (Molecular Dynamics). No product was detected, even though we could detect a minimum of 144 cpm of authentic 5′-labeled product against a background of the same amount of unincubated substrate. The second-order rate constant, k_{OH}, for hydrolysis of *N*-methylacetamide at 25°C was 3.0×10^{-4} M^{-1} min^{-1} [T. Yamana, Y. Mizukami, A. Tsuji, Y. Yasuda, K. Masuda, *Chem. Pharm. Bull.* **20**, 881 (1970)]. At pH 7.5 and 25°C, the pseudo–first-order rate constant was 9.4×10^{-11} min^{-1}. Hydrolysis of the unusually reactive Phe-Gly peptide linkage of Phe-Phe-Phe-Gly, attached by the NH_2-terminal Phe to a polyacrylamide resin, occurred at a rate of 2×10^{-7} min^{-1} at pH 7.0 and 25°C [D. Kahne and W. C. Still, *J. Am. Chem. Soc.* **110**, 7529 (1988)]. Hydrolysis of either Phe-Phe linkage could not be detected under these conditions, occurring at a rate $< 2 \times 10^{-9}$ min^{-1}.
21. Amino acid–containing substrates were prepared by chemical aminoacylation of [5′-^{32}P]$DNA1_{NH_2}$ in aqueous solution with carbonyldiimidazole as a condensing agent [K. W. Ehler and L. E. Orgel, *Biochim. Biophys. Acta* **434**, 233 (1976)]. Reaction conditions were as follows: 1 μM [5′-^{32}P]$DNA1_{NH_2}$, 0.1 M amino acid, and 0.2 M carbonyldiimidazole, freshly prepared in 0.5 M imidazole buffer (pH 8.0) and incubated at 4°C for 1 hour. Compounds corresponding to addition of one or more amino acids were separated by electrophoresis in a 20% polyacrylamide–8 M urea gel [G. Zieboll and L. E. Orgel, *J. Mol. Evol.* **38**, 561 (1994)], eluted from the gel, and purified by reversed-phase chromatography and a second round of denaturing PAGE and reversed-phase chromatography.
22. S. J. Benkovic, J. A. Adams, C. L. Borders Jr., K. D. Janda, R. A. Lerner, *Science* **250**, 1135 (1990).
23. B. L. Iverson and R. A. Lerner, *ibid.* **243**, 1184 (1989).
24. M. T. Martin, *et al.*, *J. Am. Chem. Soc.* **116**, 6508 (1994).
25. H. F. Noller, *Nature* **353**, 302 (1991).
26. S. L. Beaucage and M. H. Caruthers, *Tetrahedron Lett.* **22**, 1859 (1981).
27. We thank R. Lerner, D. Herschlag, and the members of our laboratory for helpful suggestions; U. Pieles (Ciba-Geigy) for synthesis and initial purification of the DNA-flanked amide substrates; and J. Tsang for providing evolved ribozyme G27-48. Supported by the NASA Specialized Center for Research and Training (NSCORT) in Exobiology (grant NAGW-2881).

23 September 1994; accepted 23 November 1994

Metabolic Engineering of a Pentose Metabolism Pathway in Ethanologenic *Zymomonas mobilis*

Min Zhang, Christina Eddy,* Kristine Deanda, Mark Finkelstein, Stephen Picataggio†

The ethanol-producing bacterium *Zymomonas mobilis* was metabolically engineered to broaden its range of fermentable substrates to include the pentose sugar xylose. Two operons encoding xylose assimilation and pentose phosphate pathway enzymes were constructed and transformed into *Z. mobilis* in order to generate a strain that grew on xylose and efficiently fermented it to ethanol. Thus, anaerobic fermentation of a pentose sugar to ethanol was achieved through a combination of the pentose phosphate and Entner-Doudoroff pathways. Furthermore, this strain efficiently fermented both glucose and xylose, which is essential for economical conversion of lignocellulosic biomass to ethanol.

The rapid and efficient fermentation of the pentose sugars found in lignocellulosic feedstocks is an absolute requirement for the economical conversion of biomass to ethanol. Lignocellulosic feedstocks, such as agricultural and forestry residues, are composed principally of cellulose, hemicellulose, and lignin. While there are microorganisms that efficiently ferment the glucose derived from cellulose, the conversion of the pentose sugars prevalent in hemicellulose to ethanol has been difficult because a suitable biocatalyst has not been available (*1*). Consequently, the discovery and development of microorganisms capable of converting pentose sugars, particularly xylose, to ethanol has been the focus of much research during the past 20 years. Recently, *Escherichia coli* and *Klebsiella oxytoca* have been successfully engineered for this purpose by the addition of genes for ethanol production from *Zymomonas mobilis*. In spite of the development of microorganisms with improved fermentation performance (*2*–*6*), high ethanol yields and concentrations from lignocellulosic feedstocks and short fermentation times have yet to be achieved.

Zymomonas mobilis is a bacterium that has been used as a natural fermentative agent in alcoholic beverage production. This organism demonstrates many of the traits sought in an ideal biocatalyst for fuel ethanol production, such as high ethanol yield and tolerance, high fermentation selectivity and specific productivity, the ability to ferment sugars at low pH, and considerable tolerance to the inhibitors found in lignocellulosic hydrolysates. In addition, the distillers dried grain from a *Zymomonas* fermentation is generally recognized as safe (GRAS) for use as an animal feed. Comparative performance trials have suggested that *Zymomonas* may become an important fuel ethanol–producing microorganism because it achieves 5 to 10% higher yield and up to fivefold higher volumetric productivity when compared with traditional yeast fermentations (*7*). Despite these potential advantages, fermentation processes using *Zymomonas* are still considered an immature technology compared with the industrial practice of yeast fermentation and have yet to be commercialized for fuel ethanol production from starch-based feedstocks.

Zymomonas mobilis has demonstrated ethanol yields of up to 97% of theoretical yield and ethanol concentrations of up to 12% (w/v) in glucose fermentations (*8*). These notably high yields have been attributed to reduced biomass formation during fermentation: whereas yeast produces 2 mol of adenosine triphosphate (ATP) per mole of glucose through the Embden-Meyerhoff-Parnas pathway, *Zymomonas* ferments glucose through the Entner-Doudoroff pathway (Fig. 1) and produces only 1 mol of ATP per mole of glucose (*9*, *10*). *Zymomonas*' facilitated diffusion sugar transport system (*11*) coupled with its highly expressed pyruvate decarboxylase and alcohol dehydrogenase genes (*12*) enable rapid and efficient conversion of glucose to ethanol. However, *Z. mobilis* can only ferment glucose, sucrose, and fructose and lacks the pentose metabolism pathways necessary to ferment the xylose commonly found in hemicellulose. Consequently, metabolic engineering of xylose fermentation in *Z. mobilis* is an essential step toward its development as a biocatalyst for fuel ethanol production from lignocellulosic feedstocks.

National Renewable Energy Laboratory, Applied Biological Sciences Branch, Golden, CO 80401, USA.

*Present address: Biology Department, Skidmore College, Saratoga Springs, NY 12866, USA.
†To whom correspondence should be addressed.